Science Advances
AAAS

advances.sciencemag.org/cgi/content/full/6/47/eabb7132/DC1

Supplementary Materials for

Dynamic polaronic screening for anomalous exciton spin relaxation in two-dimensional lead halide perovskites

Weijian Tao, Qiaohui Zhou, Haiming Zhu*

*Corresponding author. Email: hmzhu@zju.edu.cn

Published 20 November 2020, *Sci. Adv.* **6**, eabb7132 (2020)
DOI: 10.1126/sciadv.abb7132

This PDF file includes:

Supplementary material for this article is available online
Figs. S1 to S8
Notes S1 to S5
References

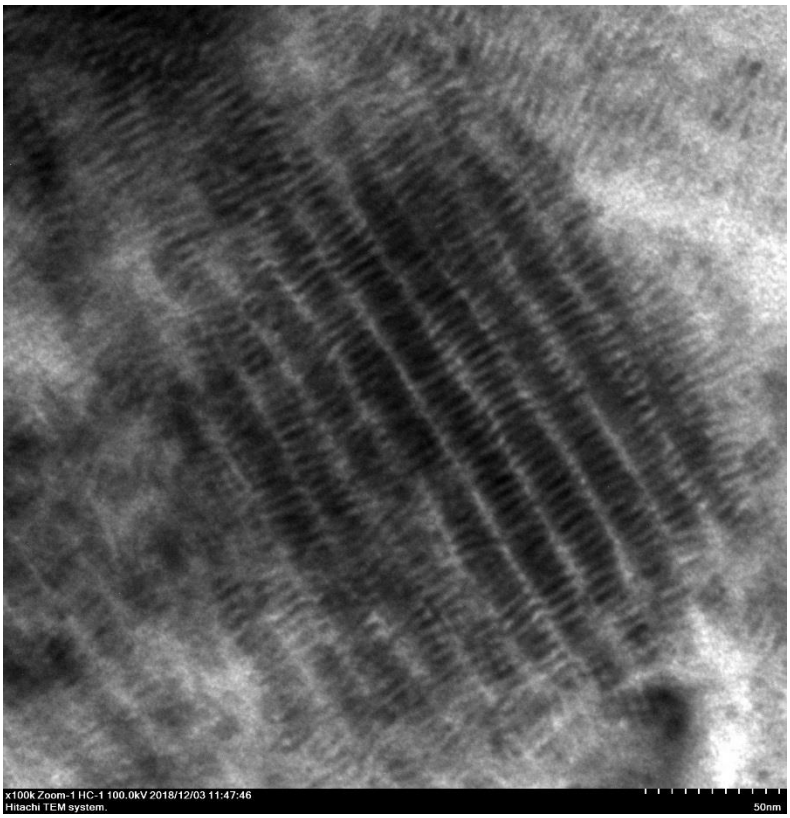

Figure S1. TEM image of the synthesized NPs which are self-assembly on copper grid in a face-to-face manner.

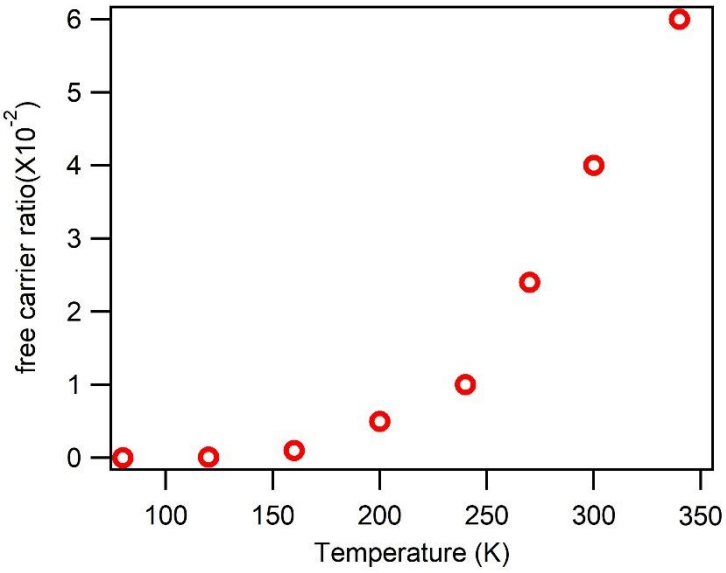

Figure S2. Estimated free carrier ratio at different lattice temperature based on Saha-Langmuir equation

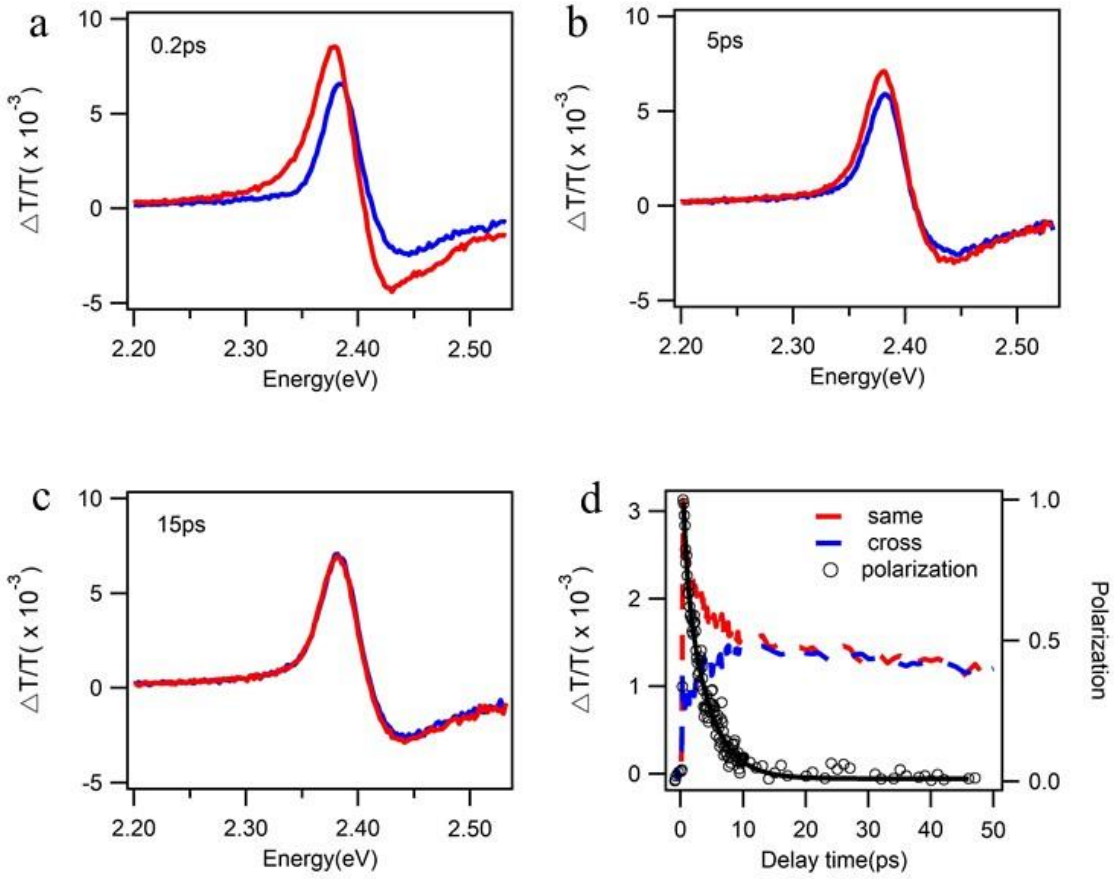

Figure S3. Spin Depolarization process in 3D $CsPbBr_3$ bulk film. (a-c) Spectral evolution for same and opposite pump-probe configuration at different pump-probe time delay (0.2 ps,5 ps,15 ps, respectively). (d)TA dynamics for same and opposite pump-probe configurations averaged at 2.34-2.39eV. Also plotted is calculated valley polarization kinetics and its single exponential fit.

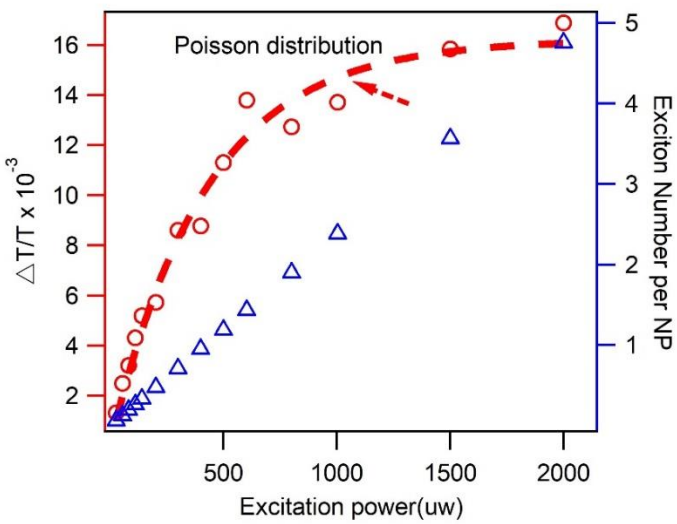

Figure S4. Estimated average exciton number per NP under different excitation power based on Poisson distribution and saturation curve.

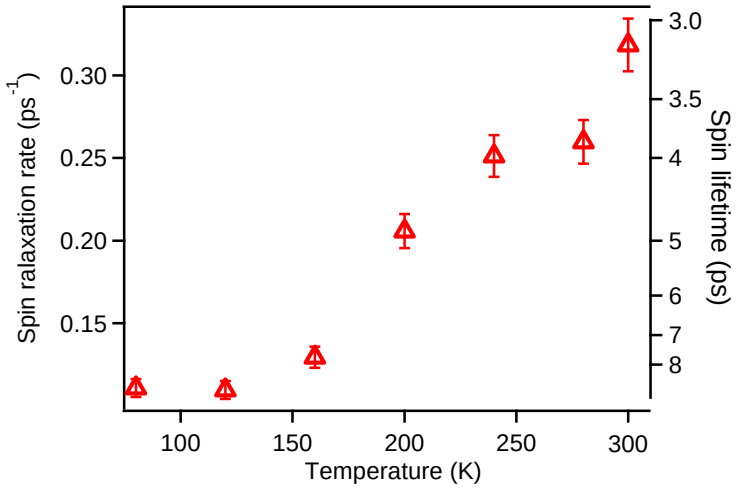

Figure S5. Spin relaxation rate as a function of temperature for 3D $CsPbBr_3$ film which shows a faster spin flip with temperature.

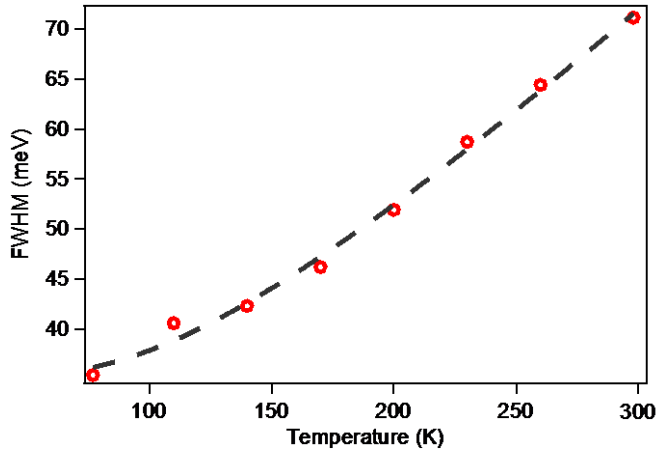

Figure S6. PL linewidth (FWHM) of 3L $CsPbBr_3$ NPs as a function of temperature. The date points can be well described with the phenomenological model shown in main text with Γ_0 = 35 meV, A = 79 meV and E_{ph} = 25 meV.

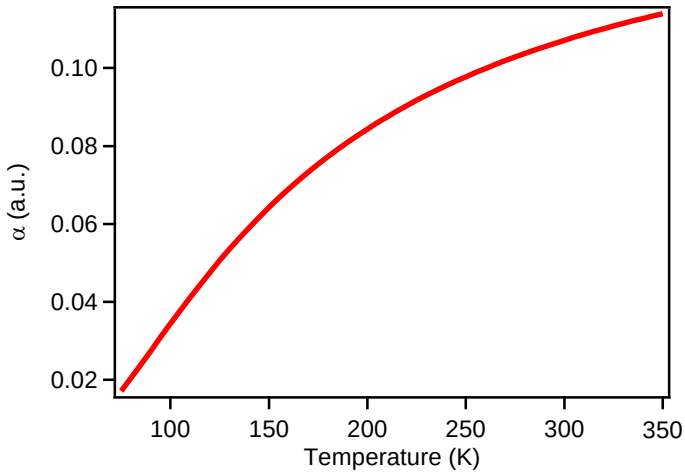

Figure S7. The dependence of polaronic coupling constant α on temperature. α increases quickly with increasing temperature in $CsPbBr_3$.

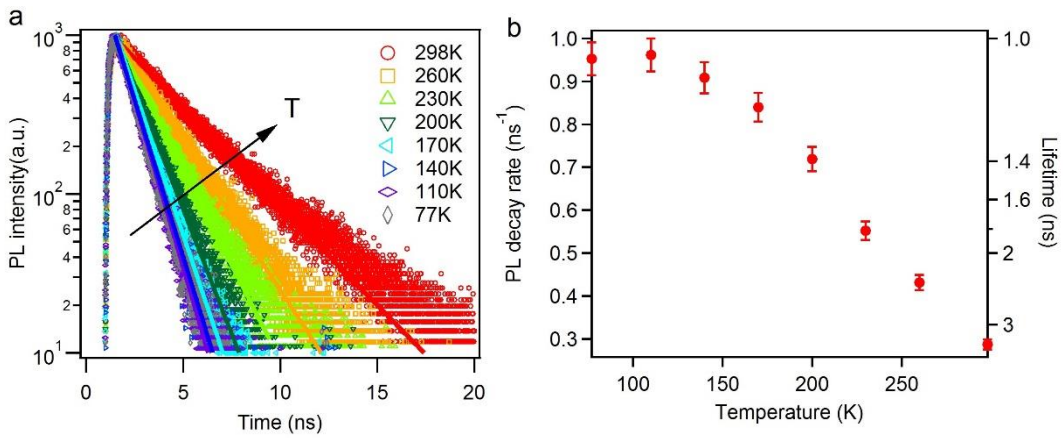

Figure S8. PL decay as a function of temperature. (a) PL decay kinetics and (b) lifetime as a function of temperature for 3L $CsPbBr_3$ NPs, showing a longer lifetime with increasing temperature.

Note S1. Estimate exciton dissociation ratio based on Saha–Langmuir equation

According to Saha-Langmuir equation, the fraction of free carrier over the total density of excitation for a 2D semiconductor, x, can be expressed as*(47)*

$$\frac{x^2}{1-x} = \frac{1}{n}\frac{\mu}{\pi\hbar^2}kTe^{\frac{-E_b}{kT}} \quad \text{(S1)}$$

where μ is exciton reduced mass which is approximated to 0.15 m_e, E_b is the exciton binding energy which is 180 meV for 3L $CsPbBr_3$. The excitation density is approximated to be an exciton per NPs, which is 10^{12} per cm^2. The temperature dependent exciton dissociation ratio can be estimated according to equation S1 and the results are present in Fig. S2. Obviously, bound exciton is the dominant (> 95%) species in the investigated temperature range.

Note S2. Excitation energy dependent initial polarization based on MSS mechanism.

According to MSS mechanism, the electron-hole exchange interaction acts as a fluctuating effect magnetic field and facilitates spin precession and the exciton spin depolarization rate can be expressed as*(14)*

$$k_s \approx \langle \Omega_K^2 \rangle \tau_p \quad \text{(S2)}$$

where $\langle \Omega_K^2 \rangle$ is the square of magnetic field averaged over exciton states which is proportional to the exciton center momentum K^2, τ_p is exciton scattering time which can be approximated to be constant at a certain temperature. Thus, we get a square relation between the exciton spin depolarization rate and exciton center momentum. $k_s \propto K^2$

Within effective mass approximation, the exciton energy and exciton center momentum obey parabolic dispersion relation, which can be expressed as

$$K = \frac{\sqrt{2\mu\varepsilon_{pump}}}{\hbar} \quad \text{(S3)}$$

where ε_{pump} is the excess energy of the pump pulse relative to the exciton resonance. Combining these relationships, we get a linear dependence of k_s on excess excitation energy.

Note S3. Estimate exciton density under different excitation power

According to Poisson distribution, the probability of generating N exciton per NP is given by $P_N = \frac{<N>^N}{N!} e^{-<N>}$ and the probability of generating not less than one exciton per NP can be expressed as

$$P_{N\geq 1} = 1 - P_0 = 1 - e^{-<N>} \quad \text{(S4)}$$

$$< N > = \sigma \cdot F \quad \text{(S5)}$$

Where <N> is the average exciton number per NP and is proportional to the absorption section σ and excitation energy.

The probability of generating not less than one exciton per NP, $P_{N\geq 1}$ can be estimated by the ground state bleach signal magnitude when the Auger recombination process completed. By fitting the bleach signal magnitude with excitation power with Poisson distribution equation, the average exciton number per NP under certain excitation power can be figured out and the result is given in Supplementary Figure 4. Together with NP lateral size, the excitation density can also be derived. We note the exciton density is averaged value.

Note S4. Another two common carrier spin relaxation mechanisms and their temperature dependence

In Maialle-Silva-Sham (MSS) mechanism, electron-hole exchange interaction flips the exciton spin as a whole.*(14)* In principle, exciton spin can be relaxed via the successive flip of either kind of carrier (electron or hole). There are two common mechanisms that can trigger carrier spin flipping process*(48)*: Elliott-Yafet (EY) and Dyakonov-Perel (DP) mechanisms. In excitonic systems, these two mechanisms lead to much slow spin flip process compared to MSS mechanism as can be inferred by orders of magnitude faster exciton spin relaxation rate than single electron/hole in TMDC and perovskites.

In Elliott-Yafet (EY) mechanism, the effective magnetic field is produced by spin-orbit interaction, which mixes wavefunctions with opposite spins. Both the electrical field produced by lattice vibrations or charged impurities can be transformed to an

effective magnetic field. Spin rotates during the collisions and the spin relaxation rate is proportional to the momentum scattering rate.

$$k_s = \chi^2 {\tau_p}^{-1} \qquad \text{(S6)}$$

where χ is the spin mixing factor and ${\tau^*}^{-1}$ is the momentum scattering rate. In nondegenerate semiconductors, $k_s \approx T^2 {\tau_p}^{-1}$ *.(48)* ${\tau_p}^{-1}$ increases with T due to phonon scattering contribution. Therefore EY mechanism would predict a faster spin relaxation rate when increasing T and has been involved to account for the thermally accelerated spin relaxation rate observed in TMDs heterostructures. EY mechanism is usually very weak in semiconductors with large bandgap.

In bulk semiconductor without central symmetry, D'yakonov-Perel' (DP) mechanism could play an important in spin relaxation process. There, the band spin degeneracy is lifted, creating an effective magnetic field and causing the spin procession. Different from EY mechanism, the spin rotates not during but between collisions. The carrier spin relaxation in 2D system can be express as *(49)*

$$k_s \approx \alpha T \tau_p \quad \text{(S7)}$$

where α is a coefficient of spin splitting, τ_p is the momentum scattering. Assuming T independent α, the T effect for DP mechanism looks very similar to MSS mechanism, except the effective magnetic field from different origins. Therefore, DP mechanism should also yield an increasing of carrier spin relaxation rate at higher temperature, as predicted by MSS mechanism.

For perovskites with centrosymmetric structure, in principle, α should be negligible and DP spin relaxation channel should be closed. But local thermal fluctuation can create dynamic symmetry breaking and Rashba effect in perovskite. *(5)* Higher temperature assists spin splitting thus larger α, activating DP spin relaxation channel. *(46)* Considering the additional T effect on α, higher T and Rashba effect should lead to faster spin relaxation, which is opposite to experimental results.

Note S5. Temperature dependent polaron coupling constant in perovskites

The strength of electron-phonon coupling in ionic crystal can be described by Fröhlich polaron coupling constant α, which is given by

$$\alpha \equiv \frac{e^2}{\hbar}\frac{1}{4\pi\varepsilon}\left(\frac{1}{\varepsilon_\infty}-\frac{1}{\varepsilon_0}\right)\sqrt{\frac{m}{2\hbar\omega}} \qquad \text{(S7)}$$

Where e is the electron charge; ε is the dielectric constant of vacuum; ε_∞ and ε_0 high frequency and low frequency dielectric constants, respectively; ω is the angular frequency of the LO phonon mode. so α is proportional to dielectric response factor $1/\bar{\varepsilon} = 1/\varepsilon_\infty - 1/\varepsilon_0$.

Both ε_∞ and ε_0 in 3D bulk $CsPbBr_3$ has been established. *(37)* The effective dielectric constant values in 2D $CsPbBr_3$ could be different. Here, we simply take the values from 3D $CsPbBr_3$ to show a general temperature effect since the main physical picture remains same. ε_∞ is 4 in $CsPbBr_3$ and ε_0 is temperature dependent due to thermally activated lattice vibration

$$\varepsilon_0 = \varepsilon_\infty + \frac{A}{\exp(\frac{E_a}{kT})-1} \qquad \text{(S8)}$$

where prefactor A = 6.5, E_a=20 meV. *(37)*

The prefactor A in perovskite is nearly 4-5 orders of magnitude larger than conventional inorganic semiconductors due to large anharmonicity. *(37)* Therefore, ε_0 shows strong dependence on temperature, which has to be considered. Since ε_0 increases with temperature, the polaron coupling constant α also increase with the temperature monotonically, as shown in Fig. S7.

REFERENCES AND NOTES

1. J.-C. Blancon, H. Tsai, W. Nie, C. C. Stoumpos, L. Pedesseau, C. Katan, M. Kepenekian, C. M. Soe, K. Appavoo, M. Y. Sfeir, S. Tretiak, P. M. Ajayan, M. G. Kanatzidis, J. Even, J. J. Crochet, A. D. Mohite, Extremely efficient internal exciton dissociation through edge states in layered 2D perovskites. *Science* **355**, 1288–1292 (2017).

2. H. Ren, S. Yu, L. Chao, Y. Xia, Y. Sun, S. Zuo, F. Li, T. Niu, Y. Yang, H. Ju, B. Li, H. Du, X. Gao, J. Zhang, J. Wang, L. Zhang, Y. Chen, W. Huang, Efficient and stable Ruddlesden–Popper perovskite solar cell with tailored interlayer molecular interaction. *Nat. Photonics* **14**, 154–163 (2020).

3. J.-C. Blancon, A. V. Stier, H. Tsai, W. Nie, C. C. Stoumpos, B. Traoré, L. Pedesseau, M. Kepenekian, F. Katsutani, G. T. Noe, J. Kono, S. Tretiak, S. A. Crooker, C. Katan, M. G. Kanatzidis, J. J. Crochet, J. Even, A. D. Mohite, Scaling law for excitons in 2D perovskite quantum wells. *Nat. Commun.* **9**, 2254 (2018).

4. C. M. Mauck, W. A. Tisdale, Excitons in 2D organic–inorganic halide perovskites. *Trends Chem.* **1**, 380–393 (2019).

5. O. Yaffe, Y. Guo, L. Z. Tan, D. A. Egger, T. Hull, C. C. Stoumpos, F. Zheng, T. F. Heinz, L. Kronik, M. G. Kanatzidis, J. S. Owen, A. M. Rappe, M. A. Pimenta, L. E. Brus, Local polar fluctuations in lead halide perovskite crystals. *Phys. Rev. Lett.* **118**, 136001 (2017).

6. A. J. Neukirch, W. Nie, J. C. Blancon, K. Appavoo, H. Tsai, M. Y. Sfeir, C. Katan, L. Pedesseau, J. Even, J. J. Crochet, G. Gupta, A. D. Mohite, S. Tretiak, Polaron stabilization by cooperative lattice distortion and cation rotations in hybrid perovskite materials. *Nano Lett.* **16**, 3809–3816 (2016).

7. K. Miyata, D. Meggiolaro, M. T. Trinh, P. P. Joshi, E. Mosconi, S. C. Jones, F. De Angelis, X.-Y. Zhu, Large polarons in lead halide perovskites. *Sci. Adv.* **3**, e1701217 (2017).

8. F. Ambrosio, J. Wiktor, F. De Angelis, A. Pasquarello, Origin of low electron–hole recombination rate in metal halide perovskites. *Energ. Environ. Sci.* **11**, 101–105 (2018).

9. D. Meggiolaro, F. Ambrosio, E. Mosconi, A. Mahata, F. De Angelis, Polarons in metal halide perovskites. *Adv. Energy Mater.* **n/a**, 1902748 (2019).

10. F. Zheng, L.-w. Wang, Large polaron formation and its effect on electron transport in hybrid perovskites. *Energ. Environ. Sci.* **12**, 1219–1230 (2019).

11. H. Zhu, K. Miyata, Y. Fu, J. Wang, P. P. Joshi, D. Niesner, K. W. Williams, S. Jin, X.-Y. Zhu,

Screening in crystalline liquids protects energetic carriers in hybrid perovskites. *Science* **353**, 1409–1413 (2016).

12. F. Thouin, D. Cortecchia, A. Petrozza, A. R. Srimath Kandada, C. Silva, Enhanced screening and spectral diversity in many-body elastic scattering of excitons in two-dimensional hybrid metal-halide perovskites. *Phys. Rev. Res.* **1**, 032032 (2019).

13. F. Thouin, D. A. Valverde-Chávez, C. Quarti, D. Cortecchia, I. Bargigia, D. Beljonne, A. Petrozza, C. Silva, A. R. Srimath Kandada, Phonon coherences reveal the polaronic character of excitons in two-dimensional lead halide perovskites. *Nat. Mater.* **18**, 349–356 (2019).

14. M. Z. Maialle, E. A. de Andrada e Silva, L. J. Sham, Exciton spin dynamics in quantum wells. *Phys. Rev. B* **47**, 15776–15788 (1993).

15. S. Konabe, Screening effects due to carrier doping on valley relaxation in transition metal dichalcogenide monolayers. *Appl. Phys. Lett.* **109**, 073104 (2016).

16. Y. Wu, C. Wei, X. Li, Y. Li, S. Qiu, W. Shen, B. Cai, Z. Sun, D. Yang, Z. Deng, H. Zeng, In situ passivation of $PbBr_6^{4-}$ octahedra toward blue luminescent $CsPbBr_3$ nanoplatelets with near 100% absolute quantum yield. *ACS Energy Lett.* **3**, 2030–2037 (2018).

17. B. J. Bohn, Y. Tong, M. Gramlich, M. L. Lai, M. Döblinger, K. Wang, R. L. Z. Hoye, P. Müller-Buschbaum, S. D. Stranks, A. S. Urban, L. Polavarapu, J. Feldmann, Boosting tunable blue luminescence of halide perovskite nanoplatelets through postsynthetic surface trap repair. *Nano Lett.* **18**, 5231–5238 (2018).

18. E. Shi, S. Deng, B. Yuan, Y. Gao, Akriti, L. Yuan, C. S. Davis, D. Zemlyanov, Y. Yu, L. Huang, L. Dou, Extrinsic and dynamic edge states of two-dimensional lead halide perovskites. *ACS Nano* **13**, 1635–1644 (2019).

19. P. Odenthal, W. Talmadge, N. Gundlach, R. Wang, C. Zhang, D. Sun, Z.-G. Yu, Z. Valy Vardeny, Y. S. Li, Spin-polarized exciton quantum beating in hybrid organic–inorganic perovskites. *Nat. Phys.* **13**, 894–899 (2017).

20. D. Giovanni, H. Ma, J. Chua, M. Grätzel, R. Ramesh, S. Mhaisalkar, N. Mathews, T. C. Sum, Highly spin-polarized carrier dynamics and ultralarge photoinduced magnetization in $CH_3NH_3PbI_3$ perovskite thin films. *Nano Lett.* **15**, 1553–1558 (2015).

21. D. Giovanni, W. K. Chong, Y. Y. F. Liu, H. A. Dewi, T. Yin, Y. Lekina, Z. X. Shen, N. Mathews, C. K. Gan, T. C. Sum, Coherent spin and quasiparticle dynamics in solution-processed layered 2D lead

halide perovskites. *Adv. Sci.* **5**, 1800664 (2018).

22. M. J. Snelling, P. Perozzo, D. C. Hutchings, I. I. Galbraith, A. Miller, Investigation of excitonic saturation by time-resolved circular dichroism in GaAs-$Al_xGa_{1-x}As$ multiple quantum wells. *Phys. Rev. B* **49**, 17160–17169 (1994).

23. D. Robart, T. Amand, X. Marie, M. Brousseau, J. Barrau, G. Bacquet, Exciton–exciton interaction under elliptically polarized light excitation. *J. Opt. Soc. Am. B* **13**, 1000–1008 (1996).

24. L. Muñoz, E. Pérez, L. Viña, K. Ploog, Spin relaxation in intrinsic GaAs quantum wells: Influence of excitonic localization. *Phys. Rev. B* **51**, 4247–4257 (1995).

25. C. R. Zhu, K. Zhang, M. Glazov, B. Urbaszek, T. Amand, Z. W. Ji, B. L. Liu, X. Marie, Exciton valley dynamics probed by Kerr rotation inWSe_2 monolayers. *Phys. Rev. B* **90**, 161302 (2014).

26. T. Yu, M. W. Wu, Valley depolarization due to intervalley and intravalley electron-hole exchange interactions in monolayerMoS_2. *Phys. Rev. B* **89**, 205303 (2014).

27. Y. Miyauchi, S. Konabe, F. Wang, W. Zhang, A. Hwang, Y. Hasegawa, L. Zhou, S. Mouri, M. Toh, G. Eda, K. Matsuda, Evidence for line width and carrier screening effects on excitonic valley relaxation in 2D semiconductors. *Nat. Commun.* **9**, 2598 (2018).

28. H. Zeng, J. Dai, W. Yao, D. Xiao, X. Cui, Valley polarization in MoS_2 monolayers by optical pumping. *Nat. Nanotechnol.* **7**, 490–493 (2012).

29. T. Amand, D. Robart, X. Marie, M. Brousseau, P. Le Jeune, J. Barrau, Spin relaxation in polarized interacting exciton gas in quantum wells. *Phys. Rev. B* **55**, 9880–9896 (1997).

30. F. Mahmood, Z. Alpichshev, Y.-H. Lee, J. Kong, N. Gedik, Observation of exciton–exciton interaction mediated valley depolarization in monolayer $MoSe_2$. *Nano Lett.* **18**, 223–228 (2018).

31. A. Chernikov, T. C. Berkelbach, H. M. Hill, A. Rigosi, Y. Li, O. B. Aslan, D. R. Reichman, M. S. Hybertsen, T. F. Heinz, Exciton binding energy and nonhydrogenic rydberg series in monolayer WS_2. *Phys. Rev. Lett.* **113**, 076802 (2014).

32. K. He, N. Kumar, L. Zhao, Z. Wang, K. F. Mak, H. Zhao, J. Shan, Tightly bound excitons in monolayer WSe_2. *Phys. Rev. Lett.* **113**, 026803 (2014).

33. S. Deng, E. Shi, L. Yuan, L. Jin, L. Dou, L. Huang, Long-range exciton transport and slow annihilation in two-dimensional hybrid perovskites. *Nat. Commun.* **11**, 664 (2020).

34. X. Chen, H. Lu, Z. Li, Y. Zhai, P. F. Ndione, J. J. Berry, K. Zhu, Y. Yang, M. C. Beard, Impact of layer thickness on the charge carrier and spin coherence lifetime in two-dimensional layered perovskite single crystals. *ACS Energy Lett.* **3**, 2273–2279 (2018).

35. C. Huo, C. F. Fong, M.-R. Amara, Y. Huang, B. Chen, H. Zhang, L. Guo, H. Li, W. Huang, C. Diederichs, Q. Xiong, Optical spectroscopy of single colloidal $CsPbBr_3$ perovskite nanoplatelets. *Nano Lett.* **20**, 3673–3680 (2020).

36. Z. Guo, X. Wu, T. Zhu, X. Zhu, L. Huang, Electron–phonon scattering in atomically thin 2D perovskites. *ACS Nano* **10**, 9992–9998 (2016).

37. Y. Guo, O. Yaffe, T. D. Hull, J. S. Owen, D. R. Reichman, L. E. Brus, Dynamic emission Stokes shift and liquid-like dielectric solvation of band edge carriers in lead-halide perovskites. *Nat. Commun.* **10**, 1175 (2019).

38. S. Dal Conte, F. Bottegoni, E. A. A. Pogna, D. De Fazio, S. Ambrogio, I. Bargigia, C. D'Andrea, A. Lombardo, M. Bruna, F. Ciccacci, A. C. Ferrari, G. Cerullo, M. Finazzi, Ultrafast valley relaxation dynamics in monolayer MoS_2 probed by nonequilibrium optical techniques. *Phys. Rev. B* **92**, 235425 (2015).

39. J. M. Kikkawa, I. P. Smorchkova, N. Samarth, D. D. Awschalom, Room-temperature spin memory in two-dimensional electron gases. *Science* **277**, 1284–1287 (1997).

40. Y. Ohno, R. Terauchi, T. Adachi, F. Matsukura, H. Ohno, Spin relaxation in GaAs(110) quantum wells. *Phys. Rev. Lett.* **83**, 4196–4199 (1999).

41. L. M. Herz, How lattice dynamics moderate the electronic properties of metal-halide perovskites. *J. Phys. Chem. Lett.* **9**, 6853–6863 (2018).

42. K. Miyata, X.-Y. Zhu, Ferroelectric large polarons. *Nat. Mater.* **17**, 379–381 (2018).

43. S. D. Stranks, P. Plochocka, The influence of the Rashba effect. *Nat. Mater.* **17**, 381–382 (2018).

44. Y. A. Bychkov, É. I. Rashba, Properties of a 2D electron-gas with lifted spectral degeneracy. *J. Exp. Theor. Phys. Lett.* **39**, 78–81 (1984).

45. S. B. Todd, D. B. Riley, A. Binai-Motlagh, C. Clegg, A. Ramachandran, S. A. March, J. M. Hoffman, I. G. Hill, C. C. Stoumpos, M. G. Kanatzidis, Z.-G. Yu, K. C. Hall, Detection of Rashba spin splitting in 2D organic-inorganic perovskite via precessional carrier spin relaxation. *APL Mater.* **7**, 081116 (2019).

46. D. Niesner, M. Hauck, S. Shrestha, I. Levchuk, G. J. Matt, A. Osvet, M. Batentschuk, C. Brabec, H. B. Weber, T. Fauster, Structural fluctuations cause spin-split states in tetragonal $(CH_3NH_3)PbI_3$ as evidenced by the circular photogalvanic effect. *Proc. Natl. Acad. Sci. U.S.A.* **115**, 9509–9514 (2018).

47. V. D'Innocenzo, G. Grancini, M. J. Alcocer, A. R. Kandada, S. D. Stranks, M. M. Lee, G. Lanzani, H. J. Snaith, A. Petrozza, Excitons versus free charges in organo-lead tri-halide perovskites. *Nat. Commun.* **5**, 3586 (2014).

48. I. Žutić, J. Fabian, S. Das Sarma, Spintronics: Fundamentals and applications. *Rev. Mod. Phys.* **76**, 323–410 (2004).